Available online at www.sciencedirect.com
SCIENCE DIRECT®
Dyes and Pigments 63 (2004) 259–276
DYES and PIGMENTS
www.elsevier.com/locate/dyepig

Theoretical molecular modelling calculations on the solid state structure of some organic pigments

D. Thetford[a,*], J. Cherryman[b], A.P. Chorlton[c], R. Docherty[d]

[a]Lubrizol Ltd, Research Department, PO Box 42, Hexagon House, Blackley, Manchester M9 8ZS, UK
[b]Avecia Ltd, Research Department, PO Box 42, Hexagon House, Blackley, Manchester M9 8ZS, UK
[c]Pharmorphix Ltd, 250 Cambridge Science Park, Milton Road, Cambridge CB1 0WE, UK
[d]Pfizer Central Research, Sandwich, Kent CT13 9NJ, UK

Received 22 December 2003; received in revised form 1 March 2004; accepted 12 March 2004

Abstract

Crystal packing calculations have been carried out on a number of commercially important organic pigments in an attempt to determine the important interactions and structural features holding pigment molecules together in selected arrangements in the solid state. The high performance pigments were found to be those with the most efficient packing and with the highest lattice energies. The most important intermolecular interactions identified were π–π stacking forces, traditional hydrogen bonds and weak hydrogen bonds.

Keywords: Molecular modelling; Pigments; Lattice energy; Intermolecular interactions

1. Introduction

Since Perkin discovered the dye mauveine, in 1856, the development of colour and its understanding has played a significant role in the progress of chemistry. The link between the molecular structure of a chromophore and its colour has been and remains the subject of much investigation [1]. The bias towards a molecular explanation of colour is understandable as in many cases the spectrum of a molecule does not differ between the gas, solution and solid phases. An important exception to this trend occurs in the area of pigments and photosensitive charge generation materials [2]. Aggregation effects may change the colour of a pigment and in the case of charge generation materials, certain lattice effects may modify the performance of the device by affecting the photogeneration efficiencies. It is naturally of considerable importance to understand the inter-relationship between crystal packing tendencies and wavelength shift. The aim is ultimately to relate packing motifs to changes in colour and photogeneration behaviour.

The consequences of this solid state effect on the development of new pigments and photosensitive materials are profound. It is no longer sufficient for the organic chemist to synthesise new

* Corresponding author. Lubrizol Ltd, Research Department, PO Box 42, Hexagon House, Blackley, Manchester M9 8ZS, UK. Tel.: +44-161-721-1401; fax: +44-161-721-5205.
E-mail address: dthe@lubrizol-additives.com (D. Thetford).

0143-7208/$ - see front matter © 2004 Elsevier Ltd. All rights reserved.
doi:10.1016/j.dyepig.2004.03.009

compounds. In addition, they must consider how these materials organise themselves in the solid state and how to control that organisation. Until recently, understanding and controlling what happens in the solid state has remained an art, but much progress has been made in crystal engineering [3–6], polymorph control [7,8], lattice energy calculations [9], structure determination from small crystals and powders [10], and ab initio structure prediction [11].

A pigment is a coloured, black, white or fluorescent particulate organic or inorganic solid which is usually insoluble in its application media. A pigment will retain its own unique crystalline or particulate structure throughout the application or incorporation process. The properties of a pigment including colour, thermal stability, particle shape, light fastness, fluorescence and bleeding characteristics are often dependant on the crystal packing arrangements of the pigment [12].

Specific arrangements or orientations adopted by molecules in the solid state are dependant on the possible interactions between molecules. Intermolecular forces are a result of the collective atom–atom interactions which depend on molecular structure. The molecules will attempt to achieve the arrangements which will result in the greatest intermolecular interactions and consequently, the maximum lattice energy.

Through carrying out an analysis of a representative collection of organic pigments (**1**–**8**), see Figs. 1 and 2, it was hoped to obtain a greater understanding of molecular structure, crystal packing and solid state property relationships for organic pigments. The ultimate aim of such a study was to use the information in the design of pigment molecules with not only the desired molecular properties but solid state properties as well.

1.1. Background theory

The structures and crystal chemistry of organic materials and theoretical methods to determine them has been reviewed [10]. The packing coefficient (C) is a useful parameter for judging the efficiency of a molecule for using space in a given solid state arrangement. This is shown below where V_{mol} is the molecular volume, V_{cell} the unit cell volume and Z is the number of molecules in the unit cell.

$$C = (Z \times V_{mol})/V_{cell}$$

This simple model assumes that the molecules within the crystal will attempt to pack in a manner such as to minimise the amount of unoccupied space. Typical packing coefficients range from 0.6 to 0.8 for organic materials and the higher the packing coefficient, the better use of space by the molecule in the solid state is attained.

In order to attempt to quantify the roles of the different types of intermolecular interaction in crystals, the lattice energy for these systems has to be calculated and partitioned into specific intermolecular contributions. To understand the important structural features that govern the solid state, it is vital to be able to describe the interactions between molecules in the solid state in terms of

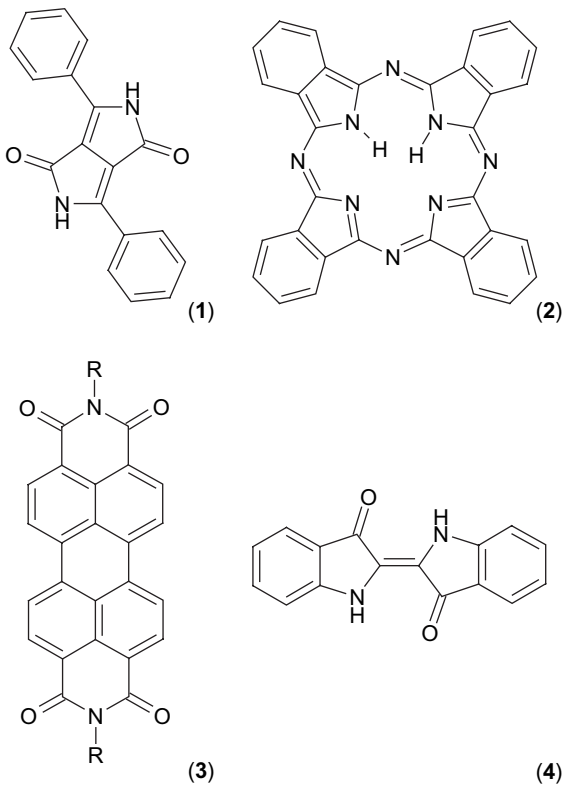

Fig. 1. The molecular structures of 1,4-diketo-pyrrolo-pyrrole **(1)**, metal free phthalocyanine **(2)**, perylene system **(3)** and indigo **(4)**.

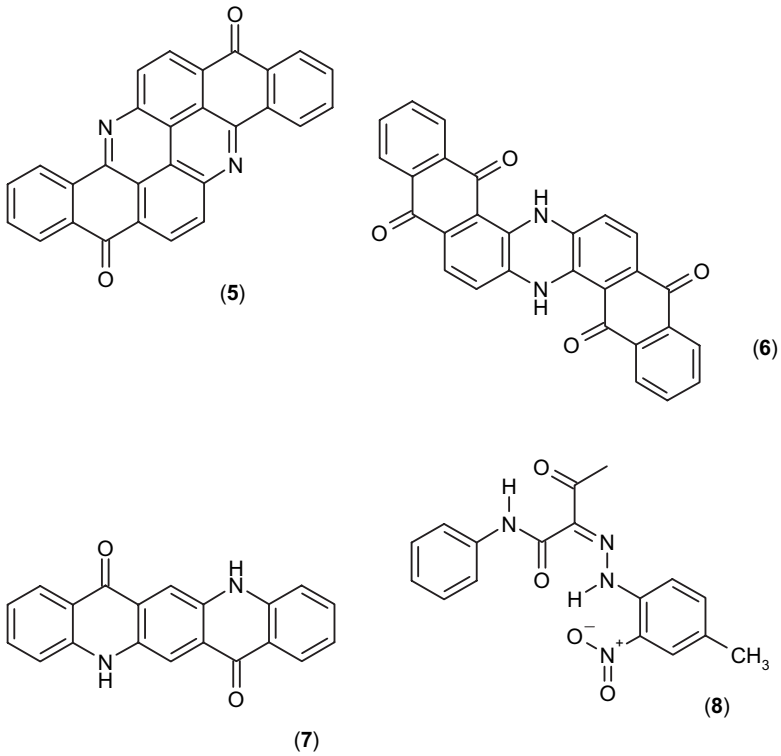

Fig. 2. The molecular structures of flavanthrone **(5)**, indanthrone **(6)**, γ-quinacridone **(7)** and CI Pigment Yellow 1 **(8)**.

energy and the specific orientations and directions. The lattice energy E_{latt}, often referred to as the crystal binding or cohesive energy, can be calculated for molecular crystals by summing all the interactions between a central molecule and all the surrounding molecules. Each intermolecular interaction can be considered to consist of the sum of the constituent atom–atom interactions [13–15]. The review by Jones and colleagues [10] explains the derivation of lattice energy in the equation, shown below.

$$E_{\text{latt}} = \frac{1}{2}\sum_{k=1}^{N}\sum_{i=1}^{n}\sum_{j=1}^{n'} V_{kij}$$

The lattice energy is a crucial parameter to calculate as this value can be compared against the sublimation enthalpy as a check of the accuracy of the potential functions and parameters employed, as evidenced from previous work [10,16]. The calculated lattice energy value has the added attraction that it may be split down into its specific intermolecular interactions and constituent atom–atom forces. This can provide a profile of the important intermolecular interactions in the solid state and an increased understanding of the specific molecular structure features and solid state property.

The importance of weak hydrogen bonds such as C–H::::O=C interactions and of Van der Waals contacts such as S::::S or Cl::::Cl, in determining the overall structural arrangements and solid state properties remains the subject of intense debate [17] and this will be considered in much greater detail for the molecules of interest in this study.

2. Experimental

The method [10] adopted for the study of the pigment systems (**1**–**8**) under investigation, is detailed below.

(a) Obtain the crystal structure of the selected compounds from the Cambridge Crystallographic Database (CCD) [18].

(b) If the structure is incomplete (ie. no hydrogens reported), then add the missing hydrogens using standard bond lengths and geometry. Unit cell volume is taken from the CCD and molecular volume was calculated using the molecular surface/Conolly surface module in CERIUS 2 [19].
(c) The partial charges on the atoms in the molecules which help describe the electrostatic contribution to the lattice energy, are calculated using a semi-empirical molecular approach (MOPAC) [20].
(d) Packing calculations are carried out using HABIT [21]. This particular program has been specifically developed for carrying out calculations of this type on organic materials.
(e) This program also allows the lattice energy to be broken down into the important intermolecular interactions and the constituent atom–atom contributions.

The actual results are considered in the next section for each system under investigation.

3. Results and discussion

3.1. 1,4-Diketo-pyrrolo-(3,4-c)pyrrole

The 1,4-diketo-pyrrolo-(3,4-c)pyrrole (DPP Red) system (**1**) shown in Fig. 1 is one of the most important recent developments in the pigments area of colour chemistry. Despite being of a relatively low molecular weight by pigment standards, these heterocyclic compounds are highly insoluble, crystalline materials which are thermally stable up to 400 °C [22]. Varying the substitiuents on the phenyl groups can vary these physical properties and the colour from yellow/orange to red/blue. The physical properties are attributed to the presence of strong intermolecular bonding present in the crystal structure.

The crystal structure of the 1,4-diketo-3,6-diphenylpyrrolo-(3,4-c)pyrrole (**1**) (Pigment Red 255) has been published [23,24] and our results are based on the former publication. This shows the molecule crystallising in a triclinic space group P1 in a unit cell of dimensions $a = 3.82$, $b = 6.521$, $c = 13.571$ Å with $\alpha = 93.33°$, $\beta = 87.07°$ and $\chi = 94.99°$. The molecular structure is almost planar with the phenyl groups tilted out of the plane of the basic chromophore by about 7°. The packing coefficient was 0.72. Crystal packing calculations were carried out using the parameters of Momany et al. [25]. The calculated lattice energy was −30.7 kcal/mol and the important intermolecular interactions are tabulated below (Table 1). The *UVW* labels are essentially the translations along the unit cell axes *a*, *b*, and *c*.

The most important interactions are the π–π stacking forces in the crystallographic *a*-direction. These interactions labelled '*a*' constitute over 42% of the total lattice energy. Hydrogen bonding interactions of the type N–H:::::O=C exist between the molecules in the *ab* direction. This hydrogen bond accounts for the majority of the 3.2 kcal/mol interaction labelled '*b*'. The interaction labelled '*c*' appears to be electrostatic in nature between the polar parts of the molecule. The interactions *abc* constitute about 82% of the total energy in the solid state.

It is important to separate the major interactions in order to display and interpret the vital intermolecular interactions. These can be best described schematically. On viewing down the *c* axis (ie. in the *ab* plane), the molecules can be viewed edge on and regarded as narrow rectangles as shown in Scheme 1. The '*a*' and '*b*' interactions are clearly visible in this idealised representation. The

Table 1
The important intermolecular interactions in DPP (**1**)

U	*V*	*W*	Interaction energy (kcal/mol)	Number of interactions	Label	Type
1	0	0	−6.4	2	*a*	π–π
1	1	0	−3.2	2	*b*	Hydrogen bonding
0	1	0	−2.9	2	*c*	Electrostatic
0	1	1	−0.6	2	*d*	Van der Waals

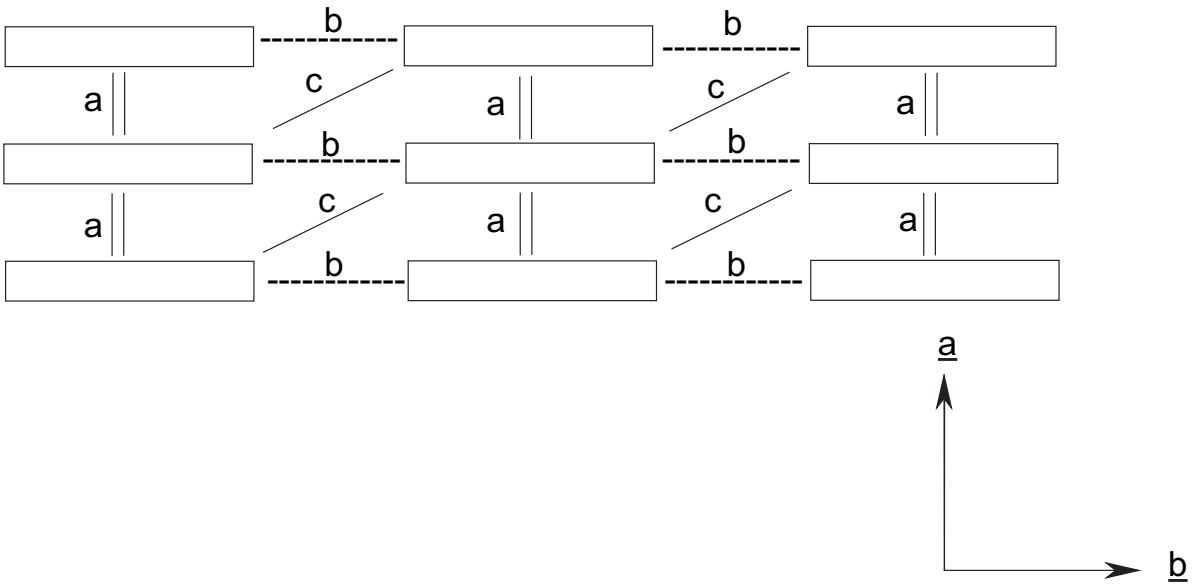

Scheme 1. Representation of the crystal packing of DPP molecules and their intermolecular interactions viewed down the *c*-axis.

'*a*' interactions are the π–π stacking forces along the *a*-direction and the '*b*' interactions are the hydrogen bonds holding the molecules together in the *b*-direction. Clearly, there is a two-dimensional stability to the structure produced by these interactions. This is supplemented by the electrostatic interactions across the *ab* diagonals.

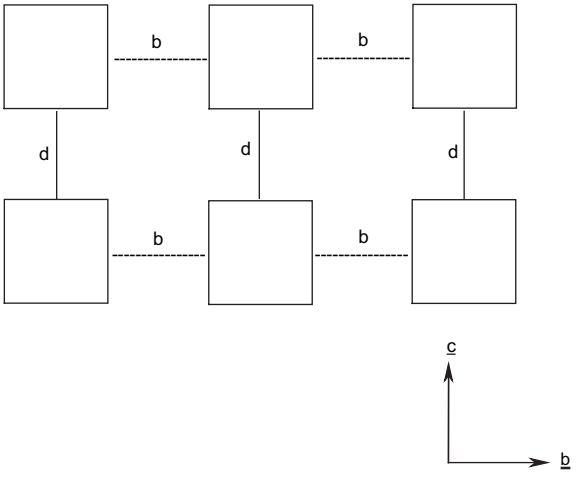

Scheme 2. Representation of the crystal packing of DPP molecules and their intermolecular interactions viewed down the *a*-axis.

If the arrangement of the molecules in Scheme 1 is viewed from above (ie. down the *a* axis, in the *bc* plane), the molecules can be considered to consist of rectangular plates as shown in Scheme 2. The important π–π interactions are now perpendicular to the plane of the paper and the hydrogen bond interactions are along the *b*-direction. The only interactions along the *c*-direction are hydrogen bonds and these are only worth 0.6 kcal/mol and this is not as strong an arrangement as described in Scheme 1. This '*d*' interaction is the weakest in Table 1 and consists largely of H:::::H non-bonded interactions. Scheme 2 is shown in terms of molecular structure in Fig. 3.

3.2. Phthalocyanines

Phthalocyanine pigments dominate the blue and green shade areas and they contribute about 25% by volume of the total world market for organic pigments. The majority of phthalocyanine pigments contain copper but a number are metal free. Particle size, shape and polymorphic form are some of the important factors that govern the properties of pigments and surface character influences colloidal behaviour such as flocculation

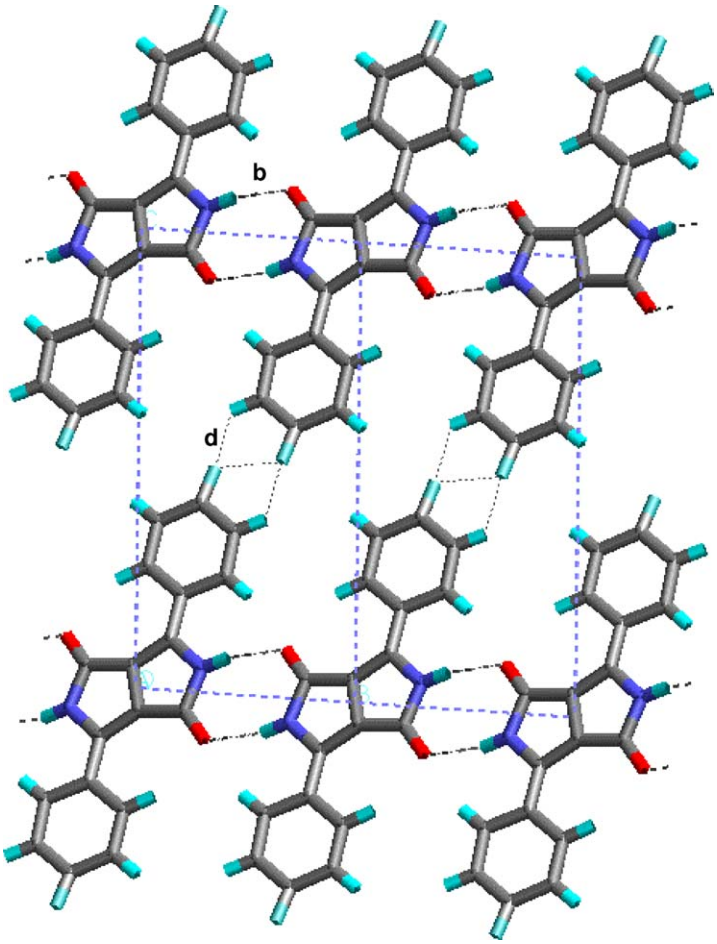

Fig. 3. The packing of DPP molecules viewed down the *a*-direction. The π–π interactions are in and out of the paper and the *b* and *d* interactions from Table 1 are labelled.

and rheological properties. The internal structure of pigment solids can influence all these properties.

The crystal structure of the β-polymorph of metal free phthalocyanine (**2**) was solved [26–28] by Robertson many years ago and shows that the planar phthalocyanine molecules crystallise in the monoclinic space group $P2_1/a$ in a unit cell of dimensions $a = 19.85$, $b = 4.72$, $c = 14.8$ Å with $\beta = 122.25°$. In fact, there are four crystal structures published in the literature [27,29–31], only one of which includes the location of the hydrogen atoms [31]. This latter publication shows that the planar phthalocyanine molecules crystallise in the monoclinic space group $P2_1/a$ in a unit cell of dimensions $a = 19.87$, $b = 4.73$, $c = 14.81$ Å with $\beta = 121.98°$ and was used to generate the following information. The β structure shows a classic herringbone arrangement with the planar molecules stacking with the faces 3.34 Å apart. The packing coefficient for the phthalocyanine molecules was 0.73. The calculated lattice energy of −42.4 kcal/mol was partitioned down into the important intermolecular interactions, see Table 2.

The most important interactions are those along the shortest crystallographic axis. These π–π stacking interactions along the *b*-axis are shown in Fig. 4, and account for 58% of the total energy in the solid state. The additional interactions are Van der Waals in nature although there appears to be some contribution from weak

Table 2
The important intermolecular interactions in phthalocyanines (**2**)

U	*V*	*W*	Interaction energy (kcal/mol)	Number of interactions	Label	Type
0	1	0	−12.4	2	*a*	π–π
1	1	0	−1.4	2	*b*	Van der Waals
1	0	0	−1.4	2	*b*	Van der Waals
0	1	1	−1.1	2	*c*	Van der Waals
1	0	1	−1.1	2	*c*	Van der Waals

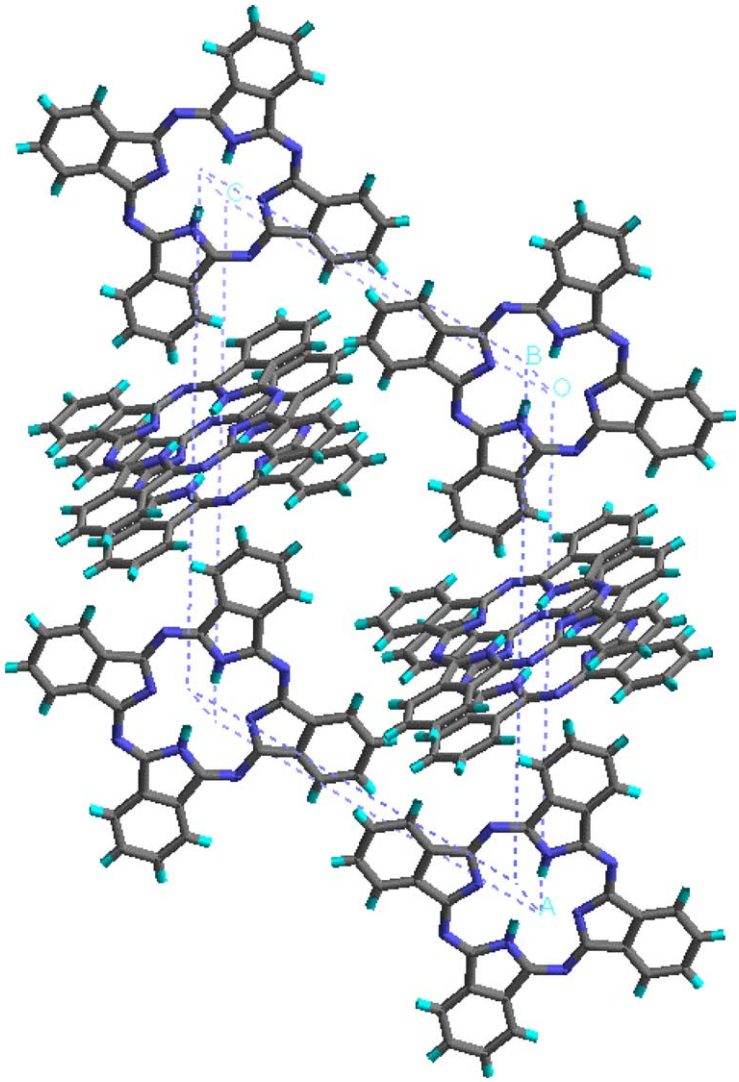

Fig. 4. The packing of phthalocyanine molecules, the stacking is along the shortest crystallographic direction. The spatial donor/acceptor arrangement is highlighted.

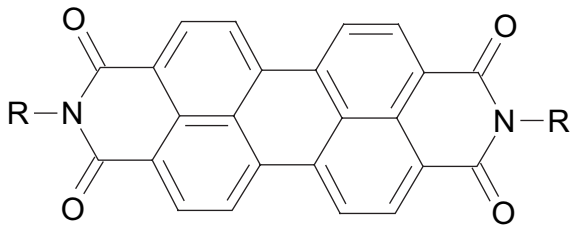

R Group	λ_{max}
CH_3	560nm
CH_2CH_3	500nm
CH_2PhOCH_3	670nm

Fig. 5. Absorption maxima for substituted perylenes.

C–H:::::N interactions. These interactions are formed when the protruding phenyl groups from a phthalocyanine molecule fits into the gaps between other phthalocyanine molecules. Each phthalocyanine molecule can be considered to consist of four spatial donors (phenyl groups) and four spatial acceptors (the gaps). These result in the eight weaker interactions shown in Table 2 and combined with the π–π interactions, account for 82% of the lattice energy.

3.3. Perylene based structures

Perylene based pigments are high performance pigments used in the automotive paint industry for predominantly the red shade area. Various substituted perylenes show roughly the same molecular absorption spectra around 530 nm but show a much wider range of absorption spectra maximum in the solid state [32,33], see Fig. 5. This change in colour from solid state effects is often referred to as crystallochromy and a detailed elegant study has been carried out on this one system over a number of years [32], with over 18 crystal structures having been solved with variations in the R group. The colour change has been correlated with crystal packing effects, in particular with the separation distance, the lateral and transverse changes in the planar part of the molecule. The molecules stack with the planar parts between 3.34 and 3.47 Å apart.

Packing calculations have been carried out on the *N*,*N*′-dimethylperylene-3,4:9,10-bis(dicarboxamide) (**3**) (where R=CH_3) (Pigment Red 179) with molecules crystallising in the monoclinic space group $P2_1/a$ with two molecules in a unit cell of dimensions $a = 3.874, b = 15.58, c = 14.597$ Å with $\beta = 97.65°$ [32]. The packing coefficient for this structure was 0.76 and the lattice energy was calculated to be −48.4 kcal/mol. The important intermolecular interactions are listed in Table 3. The most important interactions are the π–π stacking forces along the *a*-direction as these account for over half of the total lattice energy. The other interactions are a result of weak C–H:::::O=C hydrogen bonds. These and the π–π stacking interactions constitute over 80% of the lattice energy in the solid state. The important interactions are shown in Fig. 6 which shows the packing arrangement of the perylene molecules in the *bc*-plane.

3.4. Indigo

Indigo (**4**) (Pigment Blue 66) is no longer used as a commercial pigment because of its poor durability. However, it has many similar molecular features to other pigments such as quinacridones

Table 3
The important intermolecular interactions in perylenes (**3**)

U	*V*	*W*	Interaction energy (kcal/mol)	Number of interactions	Label	Type
1	0	0	−12.4	2	*a*	π–π
0	1	1	−2.4	2	*b*	C–H:::::O
0	0	1	−2.4	2	*b*	C–H:::::O
1	0	1	−1.1	2	*c*	Van der Waals
1	1	0	−1.1	2	*c*	Van der Waals

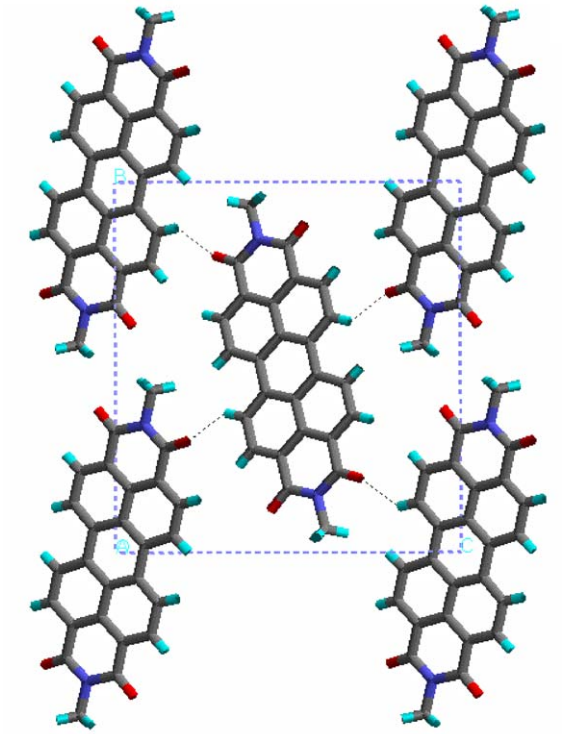

Fig. 6. The packing of perylene molecules viewed down the shortest crystallographic direction. The π–π interactions are going into the plane of the paper and the *b* interactions are shown.

and DPPs. Analysis of its packing may give some insight into the performance of indigo. Indigo and some of its derivatives show significant shifts in their solid state spectra compared to solution and vapour. This is believed to be a result of the complicated intra and intermolecular interactions present in the system. Indigo crystallises in the solid state in a monoclinic space group $P2_1/c$ in a unit cell of dimensions $a = 9.24$, $b = 5.77$, $c = 12.22$ Å with $\beta = 117°$ [34]. A full single crystal structure has been solved using synchroton radiation [35]. The use of a synchroton source results in substantially increased incident beam intensity compared to conventional laboratory source and improved resolution, especially for small crystals. As a result, the hydrogen atom positions have been located with some confidence.

The packing coefficient of indigo was 0.69 and the calculated lattice energy was −31.8 kcal/mol and was in excellent agreement with the experimental sublimation enthalpy of −32.5 kcal/mol [36]. The important interactions have been listed in Table 4. The most important interactions are the π–π stacking forces along the *b*-direction. Hydrogen bonding and electrostatic interactions provide additional stability. The weakest direction of intermolecular interactions is the *a*-axis where only weak edge to face C–H::::π interactions help to hold the molecules together in the *a*-direction. These interactions are highlighted in Fig. 7. The π–π interactions are less dominant in this structure as they only contribute 37% of the total lattice energy. The three major interactions in this system contribute 66% of the lattice energy and this is considerably less than the other examples covered in this study. This low contribution and the low packing efficiency may account for the poor durability of indigo.

3.5. Flavanthrone

Flavanthrone, Pigment Yellow 24, (**5**) is a high performance yellow pigment. The crystal structure of flavanthrone shows a planar molecule in a monoclinic space group $P2_1/a$ in a unit cell of dimensions $a = 27.92$, $b = 3.80$, $c = 8.10$ Å with $\beta = 95°$ [37]. The molecules stack at 3.44 Å apart. The packing coefficient was 0.78 and the calculated

Table 4
The important intermolecular interactions in indigo (**4**)

U	*V*	*W*	Interaction energy (kcal/mol)	Number of interactions	Label	Type
0	1	0	−5.9	2	*a*	π–π
0	1	0	−2.4	1	*b*	Hydrogen bonds
1	0	0	−2.4	1	*b*	CH–π
0	0	1	−2.3	1	*c*	Electrostatic
0	1	1	−2.3	1	*c*	Electrostatic

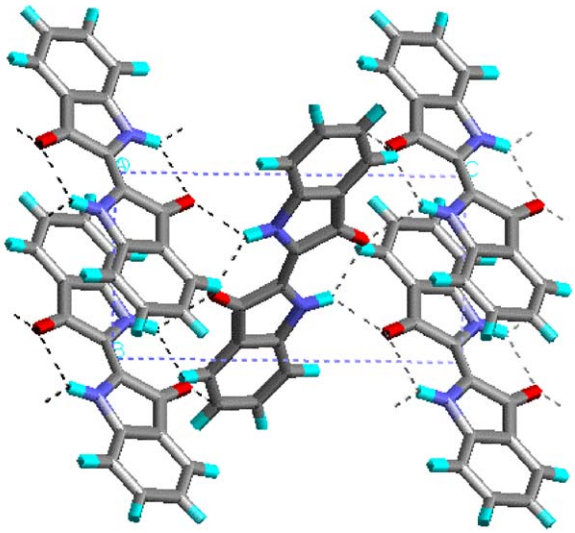

Fig. 7. The packing of indigo molecules in the solid state. The unit cell shows the hydrogen bond formation and the classic herringbone arrangement which results in aromatic edge to face interactions between molecules.

lattice energy was −43.6 kcal/mol. The important intermolecular interactions are listed in Table 5.

The most important interactions are the π–π stacking forces along the shortest crystallographic axis. These interactions correspond to 51% of the total lattice energy. The other interactions are weak hydrogen bonds of the type C–H::::O=C and appear to be slightly stronger along the *c*-axis than across the *bc* diagonal. These interactions are illustrated in Fig. 8. The weakest direction of intermolecular interactions would appear to be the *a*-axis.

3.6. Indanthrone

Indanthrone, Pigment Blue 60, (**6**) is a high performance blue pigment that is used in the automotive industry and is known to exist in a number of polymorphs. The crystal structure of the α-polymorph has been determined by Bailey [38] and shows a plate like morphology dominated by {100} and {001} faces with a more pronounced herringbone arrangement than flavanthrone. The crystal structure gives a unit cell of dimensions $a = 30.83$, $b = 3.833$, $c = 7.845$ Å with $\beta = 91.55°$. The packing coefficient of the molecule was 0.76 and the molecules are essentially planar with only small deviations from planarity. The lattice energy was calculated as −48.6 kcal/mol and was partitioned into the important intermolecular interactions listed in Table 6.

The most important interactions are those along the short *b*-axis which are π–π stacking forces. These interactions account for 56.4% of the lattice energy. The *b* and *c* interactions are weak hydrogen bonds and appear to constitute about 75% of the total lattice energy with the π–π interactions. These interactions are shown in Fig. 9.

3.7. Quinacridone

γ-Quinacridone (Pigment Violet 19), (**7**) is the most stable and commercially the most important polymorph for this structure affording a bluish red shade. The crystal structure of this polymorph has been determined by a synchrotron radiation source [39] and shows plate-like morphology in a monoclinic space group $P2_1/c$ with two molecules in a unit cell of dimensions $a = 13.761$, $b = 3.895$, $c = 13.439$ Å with $\beta = 100.33°$. The packing coefficient for this structure was 0.72 and the lattice energy was calculated to be −37.2 kcal/mol. The important intermolecular interactions are listed in Table 7.

The most important interactions are along the short *b*-axis which are π–π stacking forces and account for 45% of the lattice energy, the dimers

Table 5
The important intermolecular interactions in flavanthrone (**5**)

U	*V*	*W*	Interaction energy (kcal/mol)	Number of interactions	Label	Type
0	1	0	−11.2	2	*a*	π–π
0	0	1	−3.2	2	*b*	C–H::::O=C
0	1	1	−1.4	2	*c*	C–H::::O=C

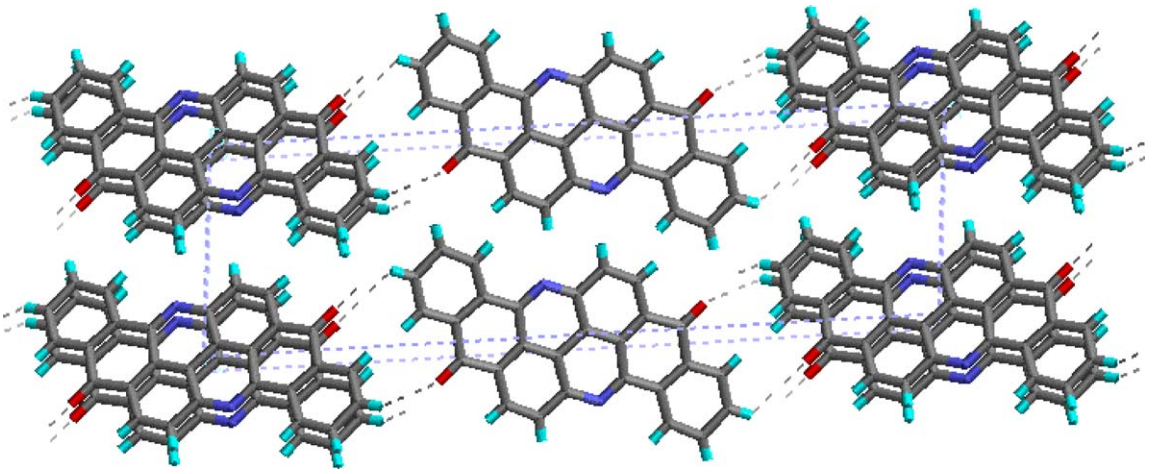

Fig. 8. The packing of flavanthrone molecules showing π–π interactions coming in and out of the paper.

having a spacing of 3.42 Å. Each quinacridone molecule has four hydrogen bonds of the type N–H::::O=C along the *c*-axis to different molecules and these constitute about 28% of the lattice energy. There are no important interactions along the crystallographic *a* direction. Fig. 10 shows a plot which combines these two important features showing the π–π stacking and hydrogen bonds. Clearly, the planar molecules are linked in sheets through hydrogen bonds but a much more complicated arrangement is involved [39] where a herringbone arrangement is visible, the angle between the planes is 78.8°. The π–π interactions in quinacridone are slightly larger than those for indigo due to the larger molecular structure producing more non-bonded interatomic contacts. The hydrogen bonds in quinacridone are also slightly stronger than in indigo which can probably be attributed to the competing intramolecular hydrogen bonds within indigo which weaken the intermolecular contacts.

3.8. CI Pigment Yellow 1

Monoazo (**8**) (Pigment Yellow 1) crystallises in the monoclinic space group $P2_1/n$ with four molecules in a unit cell of dimensions $a = 7.598$, $b = 20.375$, $c = 10.440$ Å with $\beta = 98.18°$ [40]. It has poor durability properties and is generally used in decorative paints. The packing coefficient was 0.70 and the calculated lattice energy was −37.4 kcal/mol.

The important intermolecular interactions are listed in Table 8 and account for 78% of the lattice energy. This structure is more complicated to describe because it lacks a centre of symmetry. The π–π stacking interactions and electrostatic forces combine to provide the most important interactions. The molecules are arranged in columns up the *a*-axis with subsequent molecules in an anti-parallel arrangement within these columns to maximise electrostatic interactions, see Fig. 11. The N–H groups in these molecules sit with the

Table 6
The important intermolecular interactions in indanthrone (**6**)

U	*V*	*W*	Interaction energy (kcal/mol)	Number of interactions	Label	Type
0	1	0	−13.7	2	*a*	π–π
0	1	1	−2.3	2	*b*	C–H::::O=C
0	0	1	−2.2	2	*c*	C–H::::O=C

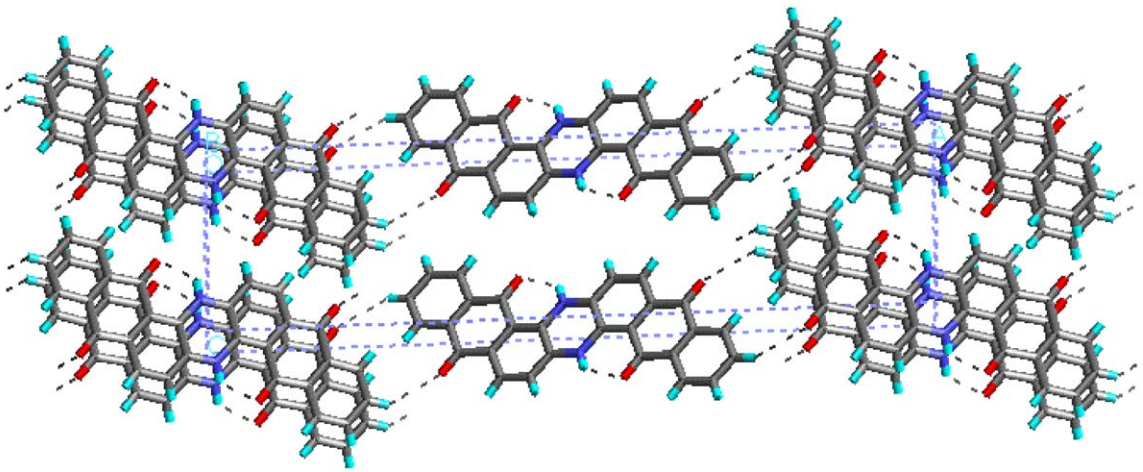

Fig. 9. The packing of indanthrone molecules showing the important interactions.

nitrogen of one molecule above the hydrogen of the previous molecule and vice versa. These columns are held together with a network of interactions of the type C–H::::O=C and C–H::::O–N roughly in the plane of the *b*-axis (parallel to the *bc*-plane). The close contacts of this type are about 2.5 Å apart.

3.9. Weak hydrogen bonds

The importance of weak hydrogen bonds of the type C–H:::::X where X=O, N, S or Cl, in determining the overall structural arrangements remains the subject of debate [17]. The weight of evidence from spectroscopic, theoretical and crystallographic studies, seem to confirm their existence as an important structural feature and that hydrogen bond is a reasonable description [41,42]. In a comprehensive study of 113 crystal structures solved by neutron diffraction, Taylor and Kennard showed that for C–H hydrogens, there is a statistically significant tendency to form short C–H:::::O non-bonded contacts. They established also that there was considerable directional preference to these interactions and that the interactions were largely electrostatic in nature. These interactions have also been the subject of considerable investigation elsewhere [17,43,44].

In our studies of the short C–H::::O contacts in perylenes, indanthrones and flavanthrones, the non-bonded contact distances vary from 2.4 to 2.53 Å, the outer limits for such contacts reported in the literature [44]. The C–H::::O contact angles vary from 132.6 to 136.2°, clearly trying to establish an ideal contact of 120° where the hydrogen atoms could align themselves with the sp2 lone pairs of the carbonyl oxygen. Further investigations on indanthrone and flavanthrone will be reported later. Some care must be taken in the interpretation of the non-bonded contact distance

Table 7
The important intermolecular interactions in quinacridone (**7**)

U	*V*	*W*	Interaction energy (kcal/mol)	Number of interactions	Label	Type
1	1	0	−8.4	1	*a*	π–π
0	−1	0	−8.4	1	*a*	π–π
0	0	0	−2.6	1	*b*	N–H::::O=C
0	−1	0	−2.6	1	*b*	N–H::::O=C
0	0	1	−2.5	1	*c*	N–H::::O=C
0	−1	1	−2.5	1	*c*	N–H::::O=C

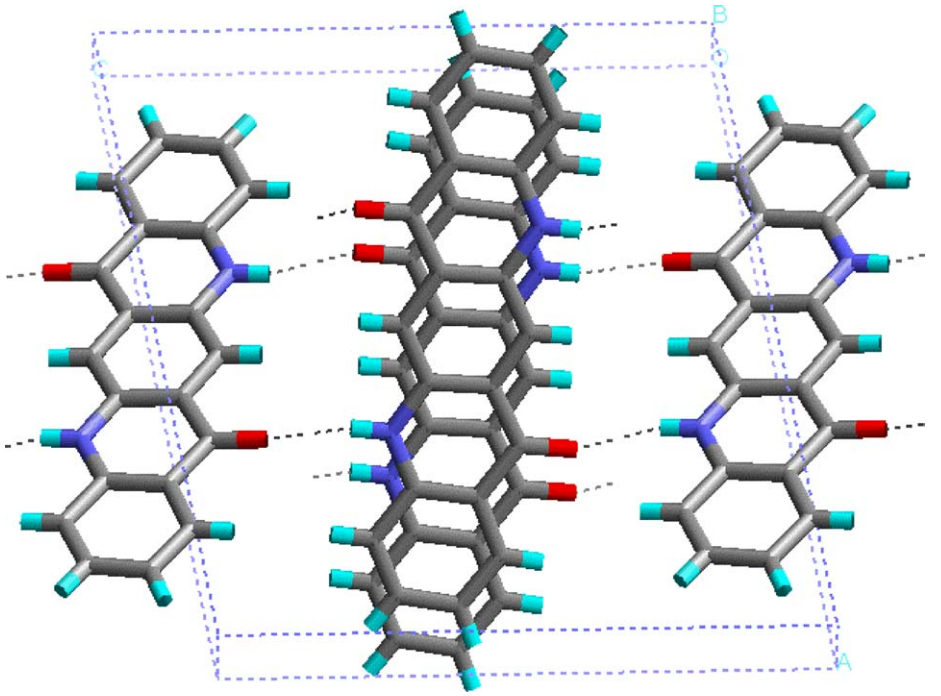

Fig. 10. The packing of χ-quinacridone molecules in which the π–π interactions are in and out of the paper.

and angles for these particular systems in this study because of the limited accuracy of the published structure determinations. However, the results are entirely consistent with more accurate studies described elsewhere [41,43].

Molecular orbital calculations using AM1 [20] have been carried out on selected structures in order to examine the magnitude of these interactions and to quantify their relative importance in the pigment structures of interest in this study. Initially, we considered the structure of benzoquinone [45] which crystallises in layers held together by dimer forming C–H::::O non-bonded contacts as shown in Fig. 12. The dimer energy from the crystal structure was found to be −3.0 kcal/mol and from the minimised gas phase structure as −3.2 kcal/mol. This is over half the energy amount of a traditional carboxylic acid dimer structure arrangement and is in excellent agreement with the estimate of an individual C–H::::O interaction being worth −1.4 kcal [18].

Next, we considered the crystal structure of acetic acid [46] which incorporates a non-traditional dimer structure (**A**) in preference to the more traditional dimer structure (**B**), see Fig. 13. Using AM1 [20], the minimised dimer arrangement based on the crystal structure has an energy of −4.1 kcal/mol whereas the minimised traditional dimer arrangement (**B**) has a dimer energy of −5.5 kcal/mol. This is in excellent agreement with

Table 8
The important intermolecular interactions in CI Pigment Yellow 1 (**8**)

U	*V*	*W*	Interaction energy (kcal/mol)	Number of interactions	Label	Type
1	1	0	−10.6	1	*a*	π–π/electrostatic
0	1	0	−9.8	1	*b*	π–π/electrostatic
1	1	1	−2.2	2	*c*	N–O::::H–C
0	1	1	−2.1	2	*c*	N–O::::H–C

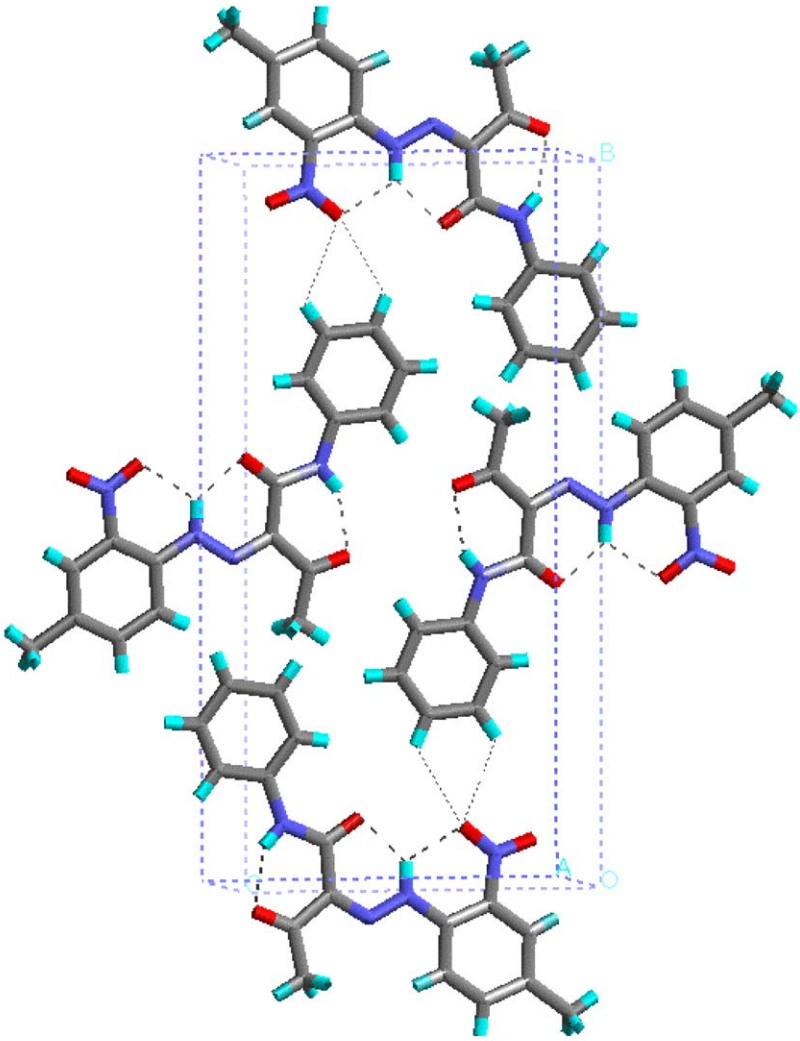

Fig. 11. The packing of CI Pigment Yellow 1 molecules.

the calculations based on atom–atom potentials [44] which resulted in dimer energies for (**A**) and (**B**) of −4.3 and −6.5 kcal/mol, respectively.

Then, we looked at the crystal structures of the 1:1 complexes of urea/barbital (**C**) and acetamide/barbital (**D**) [47,48]. The structures are isomorphous both crystallising in the orthorhombic space group $P2_12_12_1$. The unit cell dimensions are given in Fig. 14, and they are only slightly different for the two complexes, with the acetamide/barbital dimensions slightly larger in the *a* and *b* dimensions in order to incorporate acetamide which is bulkier than urea. Urea forms a bifurcated hydrogen bond with the oxygen atom in barbital. Acetamide makes similar contacts in which a C–H:::::O contact replaces an N–H:::::O contact with a retention of overall structure (space group symmetry). Molecular orbital calculations (AM1) on the crystal structures indicate a binding energy of −3.8 kcal/mol for urea/barbital and −2.4 kcal/mol for acetamide/barbital. The calculated value of −3.8 kcal/mol for the urea/barbital bifurcated

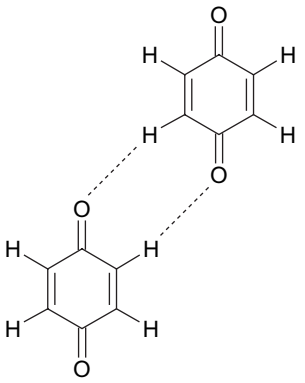

Fig. 12. Structure of benzoquinone dimer.

hydrogen bond is in excellent agreement with the urea–urea bifurcated hydrogen bond of −4.5 kcal/mol from atom–atom potential methods [49].

3.10. Intermolecular interactions involving halogens

The structure determining role of C–H::::: (Halogen) and halogen::::halogen interactions is even less well characterised than the weak hydrogen bonds but has been a matter of interest for many years. These interactions are believed to be attractive in nature [50]. In this investigation, we have restricted our studies to indigo (**4**), dichloroindigo (**9**) [51] and dibromoindigo (**10**) [52] (see Fig. 15) as these are the only systems close in structure to the pigment systems of interest and that have sufficient and accurate structural information to be of use, see Table 9.

Crystallographic studies [41] have highlighted a number of short Cl::::H contacts which are closer than the sum of the Van der Waals radii of 2.95 Å. The shortest contact reported was 2.57 Å. Theoretical calculations on chlorine containing systems have encountered problems in reproducing experimental observables and some workers

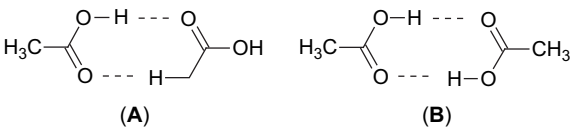

(**A**) (**B**)

Fig. 13. The dimer arrangements of acetic acid.

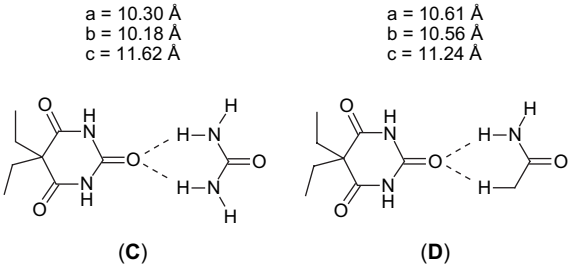

(**C**) (**D**)

Fig. 14. The crystal structures of 1:1 urea:barbital (**C**) and 1:1 acetamide:barbital (**D**) complexes.

have proposed a partial covalent bond with the strength of about 3% of a full covalent bond [53]. Others have suggested an anistropic Van der Waals radii within the potential functions [54], the Van der Waals radii would be 1.90 and 1.67 Å perpendicular and parallel to the non-bonded contact direction.

Chlorine–chlorine interactions have specific arrangements (**I** and **II**) with contact distances ranging from 3.27 to 3.49 Å, respectively, see Fig. 16. The arrangement (**I**) is consistent with an inversion centre, twofold axis or mirror plane. Due to the limited number of crystal systems adopted by organic molecules, this usually results in triclinic space groups [11].

Molecular mechanics (MM) and molecular orbital (MO) calculations have been employed to study the important interactions in the solid state structures of indigo, dichloroindigo and dibromoindigo. The default force field within SYBYL [55] has been used for MM and MOPAC [20] for MO. A lack of parameters prevented the use of the more sophisticated force fields for crystal packing calculations which were used earlier on the pigment systems of interest.

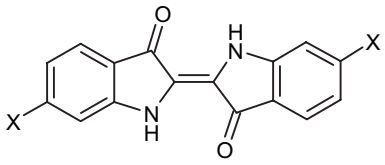

X = H (**4**)
= Cl (**9**)
= Br (**10**)

Fig. 15. The molecular structures of indigo **(4)**, 6,6′-dichloroindigo **(9)** and 6,6′-dibromoindigo **(10)**.

Table 9
The structural details for the base and halogenated indigos (**4**, **9**, **10**)

X	H	Cl	Br
Structure	Indigo	Dichloroindigo	Dibromoindigo
a	9.24	15.07	11.5
b	5.77	3.75	4.85
c	12.22	5.77	12.6
α	90	86.76	90
β	107	97.22	104
χ	90	94.5	90
Source	Ref. [29]	Ref. [45]	Ref. [46]
Crystal system	Monoclinic	Triclinic	Monoclinic
Space group	$P2_1/c$	P1	$P2_1/a$
C	0.68	0.69	0.68
Dimer energy (kcal/mol)	−6.1	−7.8	−7

The dimer energy calculated for indigo of −6.1 kcal/mol is in excellent agreement with the value of −5.9 kcal/mol calculated earlier in this study. In dichloroindigo, the dimer energy is increased to −7.8 kcal/mol. In dibromoindigo, the increase in dimer energy is only to −7.0 kcal/mol. The packing efficiency of the dichloro system is increased relative to indigo and dibromoindigo indicating a more efficient use of the space in the solid state. The *b*-axis is also the shortest in the dichloroindigo case. One of the most obvious changes in the structure for the dichloroindigo case is in the crystal system in that it has been reduced to a triclinic space group in an attempt to achieve the chlorine arrangement (**I**) discussed earlier. The Cl::::Cl contact distance is 3.44 Å and the Cl::::H dimer is 2.99 Å. The calculated interaction energies for these systems are given in Table 10.

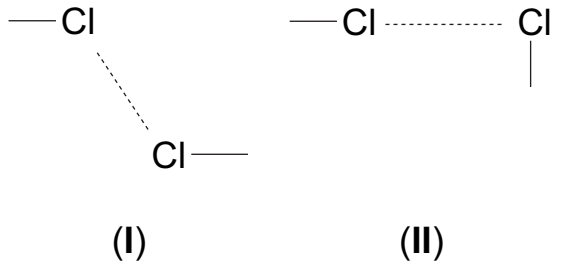

Fig. 16. Arrangements for chlorine–chlorine interactions.

These calculations suggest that the Cl::::Cl and Cl::::H interactions are relatively weak when compared against the hydrogen bond and the weak hydrogen bonds. As individual interactions, they are, however, 10 times stronger than an H::::H interaction which is worth about 0.06 kcal/mol [56]. Replacing a hydrogen atom with a chlorine atom on the end of a benzene ring is likely to increase the intermolecular interactions in that direction. In dichloroindigo, the Cl::::H and Cl::::Cl interactions along with hydrogen bonds hold the molecules together in a layer. The layers are held together through π–π stacking interactions.

4. Conclusions

Theoretical calculations have been employed to examine the important interactions in pigment type molecules. Excellent agreement was found with experimental data where for example, the calculated lattice energy of indigo is in agreement with its experimental sublimation enthalpy and the theoretical dimer energy of phthalocyanines is in agreement with the experimental dimer energy for porphyrins.

The packing coefficient (*C*) for the pigment systems studied were in general agreement with the trends discussed in earlier publications [11,13]. Large, flat aromatic systems seem to have the largest values, eg. perylene based pigment (0.76), phthalocyanine (0.73). The value of 0.76 is close to perylene itself (0.78), the slight reduction probably being due to the disruption by the end methyl groups. The high performance pigments tend to have the best packing coefficients and the values tend to be above 0.70. They also tend to have the highest lattice energies (> 40 kcal/mol) though this does depend to some extent on molecular size. The

Table 10
The important intermolecular interactions involving chlorine atoms

Non-bonded interaction	Distance (Å)	Energy (kcal/mol)	Method
Cl::::Cl	3.44	−0.50	MO
		−0.47	MM
Cl::::H	2.99	−0.45	MO
		−0.70	MM

low performance pigments such as indigo and CI Pigment Yellow 1 have lower packing values (0.68) and tend to have the lower lattice energies (30–37 kcal/mol). The packing coefficients of these two molecules are closer to those of disperse dyes than pigments [18].

The perylene based pigment studied, is interesting in that despite having weak hydrogen bond interactions present through C–H::::O=C contacts, its packing efficiency remains high. It is an attractive possibility that in certain cases, weak hydrogen bonds can be designed into the molecular framework so as to complement the desire to pack in the most efficient manner rather than compete against it as in the case of traditional hydrogen bonds. This would offer the best of both worlds.

The π–π interactions are the most important interactions dominating the majority of the structures and accounting for over 50% of the total lattice energy. In some of the larger planar systems, they can contribute up to 85% of the total lattice energy. These interactions usually occur along the shortest crystallographic axis. The desire to pack efficiently overrides all other considerations except for hydrogen bonding. The π–π interactions forming dimers in phthalocyanines have a calculated value of −12.4 kcal/mol which is in excellent agreement with the published experimental estimate of -11.4 ± 2.4 kcal/mol for the dimer energy in porphyrins [56]. In phthalocyanines, spatial donor and spatial acceptor regions have been identified.

The strengths of π–π interactions result from the collective sum of a large number of small interactions rather than one specific intermolecular interaction such as that in a traditional hydrogen bond. The structures of the systems involved, adopt similar arrangements and the planar parts of the molecule sit parallel above and below each other separated by about 3.5 Å but slipped or offset from one another. The offset is about 3 Å in phthalocyanines and 1.5 Å in perylenes, flavanthrone and indanthrone. The π–π interactions are a more complex phenomena than might first appear. They contain both Van der Waals attractive and repulsive interactions as well as an electrostatic contribution. They are actually a combination of the repulsion between the π clouds and the attraction between the π clouds and the underlying partially charged σ framework. In the comprehensive review [56] on the nature of π–π interactions, the origin of π–π stacking and the magnitude of the interactions is described in some detail with the argument that the balance of π–π repulsion and π–σ attraction governs the degree of offset.

Hydrogen bonding interactions also play an important role in holding the molecules together though not as dominant as one might initially think. Even in indigo and DPP, they are not the most important interactions in terms of magnitude. However, the need to arrange in networks does reduce the packing efficiency and so they do have a major role in overall structure arranging.

One of the more interesting observations in this study, was the role of weak hydrogen bonds in completing the three-dimensional intermolecular interactions in selected structural arrangements. The calculated interaction energies for these weak hydrogen bond dimers ranged from a half to a third as strong as conventional hydrogen bonds. Further calculations on selected systems (Section 3.9) confirmed the importance of these interactions. The role of directional contacts such as Cl::::Cl and Cl::::H non-bonded interactions were less clear but the studies in Section 3.10 seemed to indicate that the additional interactions help tighten up the packing in selected arrangements.

In such a limited analysis of poor quality structures, care must be taken in interpretation of the exact numbers produced. However, the trends from different methods and from crystallographic evidence suggest an order of relative importance and magnitude for the interactions and this is given in Table 11. Calculations and crystallography suggest that it should be possible to design potential weak hydrogen bond forming units into the molecular framework which will compliment the

Table 11
The important intermolecular interaction strengths

Interaction type	Strength (kcal/mol)
π–π dimer	−11
Traditional hydrogen bond dimer	−6
Special hydrogen bond dimer	−(2.0–3.0)
Cl::::H	−(1.0–1.5)
Cl::::Cl	−0.5
H::::H	−0.06

need for molecules to pack in the most efficient manner. However, there will always be competing interactions and packing from traditional hydrogen bonds.

References

[1] Gordon PF, Gregory P. Organic chemistry in colour. Berlin: Springer-Verlag; 1983.
[2] Herbst W, Hunger K. Industrial organic pigments: production, properties, applications. 2nd ed. Weinheim: VCH; 1997.
[3] Aakeröy CB, Seddon KR. Chem Soc Rev 1993;22(6): 397–407.
[4] Desiraju GR, editor. The crystal as a supra-molecular entity. UK: J. Wiley & Sons; 1996.
[5] Desiraju GR. Curr Sci 2001;81(8):1038–42.
[6] Lincke G. Dyes Pigments 2003;59(1):1–24.
[7] Dunitz JD, Bernstein J. Acc Chem Res 1995;28(4):193–200.
[8] Gavezzotti A, Filippini G. J Am Chem Soc 1995;117(49): 12299–305.
[9] Charlton MH, Docherty R, Hutchings MG. J Chem Soc Perkin Trans 2 1995;2023–30.
[10] Fagan PG, Hammond RB, Roberts KJ, Docherty R, Chorlton AP, Jones W, et al. Chem Mater 1995;7(12):2322–6.
[11] Docherty R, Jones W. Theoretical methods for crystal structure determination, Chapter 5. In: Jones W, editor. Organic molecular solids: properties and applications. CRC Press Inc.; 1997. p. 113–48.
[12] Langhals H, Demmig S, Potrawa T. J Prakt Chem 1991; 733–48.
[13] Kitaigorodskii AI. Physical chemistry. Molecular crystals and molecules, vol. 29. New York: Academic Press; 1973.
[14] Williams DE. J Chem Phys 1965;43(12):4424–6.
[15] Docherty R, Roberts KJ. J Cryst Growth 1988;88:159–68.
[16] Docherty R, Clydesdale G, Roberts KJ, Bennema P. J Phys D: Appl Phys 1991;24:89–99.
[17] Desiraju GR. Crystal engineering—the design of organic solids. Materials Science Monographs, No. 54. Amsterdam: Elsevier; 1989.
[18] Allen FH, Kennard O, Watson DG, Brammer L, Orpen AG, Taylor R. J Chem Soc Perkin Trans 2 1987;S1–19.
[19] CERIUS 2 Version 1.6. Biosym/Molecular Simulations, 240/250 The Quorum, Barnwell Rd, Cambridge, UK; 1995.
[20] MOPAC Version 6.0. QCPE Program 455, Quantum Chemical Program Exchange, Creative Arts Building 181, Indiana University, Bloomington, Indiana 47405; 1991.
[21] Clydesdale G, Docherty R, Roberts KJ. Comput Phys Commun 1991;64:311–28.
[22] Iqbal A. Thirteenth International conference in organic coatings science and technology 1987. In: Patsis AV, editor. Advances in organic coatings science and technology series, vol. 11. Lancaster, PA: Technomic Publication; 1989. p. 82–96.
[23] Iqbal A, Jost M, Kirchmayr R, Pfenninger J, Rochat A, Wallquist O. Bull Soc Chim Belg 1988;97(8–9):615–43.
[24] Mizuguchi J, Grubenmann A, Wooden G, Rihs G. Acta Crystallogr Sect B 1992;48(5):696–700.
[25] Momany FA, Carruthers LM, McGuire RF, Scheraga HA. J Phys Chem 1974;78(16):1595–620.
[26] Robertson JM. J Chem Soc 1935;615–21.
[27] Robertson JM. J Chem Soc 1936;1195–209.
[28] Robertson JM. J Chem Soc 1937;219–30.
[29] Zugenmaier P, Bluhm TL, Deslandes Y, Orts WJ, Hamer GK. J Mater Sci 1997;32(20):5561–8.
[30] Kubiak R, Janczak J. J Alloys Compd 1992;190(1):117–20.
[31] Matsumoto S, Matsuhama K, Mizuguchi J. Acta Crystallogr Sect C 1999;55(1):131–3.
[32] Hädicke E, Graser F. Acta Crystallogr Sect C 1986;42: 189–95.
[33] Hädicke E, Graser F. Acta Crystallogr Sect C 1986;42: 195–8.
[34] von Eller H. Bull Soc Chim Fr 1955;1433–8.
[35] Süsse P, Steins M, Kupcik V. Z Kristallogr 1988;184: 269–73.
[36] Cox JD, Pilcher G. Thermochemistry of organic and organometallic compounds. New York: Academic Press; 1970.
[37] Stadler HP. Acta Crystallogr 1953;6:540–2.
[38] Bailey M. Acta Crystallogr 1955;8:182–5.
[39] Potts GD, Jones W, Bullock JF, Andrews SJ, Maginn SJ. J Chem Soc Chem Commun 1994;2565–6.
[40] Paulus EF. Z Kristallogr 1984;167:65–72.
[41] Taylor R, Kennard O. J Am Chem Soc 1982;104(19): 5063–70.
[42] Desiraju GR. Acc Chem Res 1996;29(9):441–9.
[43] Sarma JARP, Desiraju GR. J Chem Soc Perkin Trans 2 1987;1195–202.
[44] Berkovitch-Yellin Z, Leiserowitz L. Acta Crystallogr Sect B 1984;40:159–65.
[45] Trotter J. Acta Crystallogr 1960;13:86–99.
[46] Nahringbauer I. Acta Chem Scand 1970;24(2):453–62.
[47] Gartland GL, Craven BM. Acta Crystallogr Sect B 1974; 30:980–7.
[48] Hsu IN, Craven BM. Acta Crystallogr Sect B 1974;30: 974–9.
[49] Docherty R, Roberts KJ, Saunders V, Black S, Davey RJ. Faraday Discuss 1993;95:11–25.
[50] Desiraju GR, Parthasarathy R. J Am Chem Soc 1989; 111(23):8725–6.
[51] Süsse P, Wasche R. Naturwissenschaften 1978;65:157.
[52] Süsse P, Krampe C. Naturwissenschaften 1979;66:110.
[53] Nyburg SC, Faerman CH. Acta Crystallogr Sect B 1985; 41:274–9.
[54] Williams DE, Hsu LY. Acta Crystallogr Sect A 1985;41: 296–301.
[55] Docherty R, Morley JO. Personal communication.
[56] Hunter CA, Sanders JKM. J Am Chem Soc 1990;112(14): 5525–34.